ttp

Modelling damage progression by a statistical energy-balance algorithm

Federico Bosia[1,a], Nicola Pugno[2,b], Giuseppe Lacidogna[2,c] and Alberto Carpinteri[2,d]

[1] Dipartimento di Fisica, Politecnico di Torino, Corso Duca degli Abruzzi 24, 10124 Torino

[2] Dipartimento di Ingegneria Strutturale e Geotecnica, Politecnico di Torino, Corso Duca degli Abruzzi 24, 10124 Torino

[a]federico.bosia@polito.it, [b]nicola.pugno@polito.it, [c]giuseppe.lacidogna@polito.it, [d]alberto.carpinteri@polito.it

Keywords: Acoustic Emission, Damage progression, Scaling behaviour, Modeling.

Abstract. In this contribution some characteristics and predictive capabilities are discussed of a recently introduced model for damage progression and energy release, in view of modelling Acoustic Emission. The specimen is discretized in a network of connected springs, similar to a Fibre Bundle Model approach, with the spring intrinsic strengths statistically distributed according to a Weibull distribution. Rigorous energy balance considerations allow the determination of the dissipated energy due to crack surface formation and kinetic energy propagation. Based on results of simulations, the macroscopic behaviour emerging from different choices at "mesoscopic" level is discussed, in particular the relevance of model parameters such as the distribution of spring cross sections, Weibull modulus values, and discretization parameters in determining results like stress-strain curves and energy scaling versus time or specimen size.

Introduction

Various attempts have been made in the literature to describe the qualitative and quantitative behaviour emerging in Acoustic Emission (AE) experiments (e.g. [1,2]). In most of the existing approaches, however, essential aspects of fracture mechanics are often neglected, such as energy dissipation and fracture energy balance.

Recent analysis of AE experiments has highlighted the multiscale aspect of cracking phenomena and fractal statistical analysis has been applied to describe the data, and energy dissipation has been shown to occur in a fractal domain comprised between a surface and a volume [3,4]. The aim is to introduce these aspects in a simple model that expands on the approaches appearing in the literature, and evaluate the influence of the proposed modifications on expected results.

Description of the model

To correctly describe the phenomenon of damage progression in quasistatic experiments, our goal is to introduce the simplest possible model M_0 containing the correct energetic behaviour. For the sake of simplicity, a specimen having length L_{tot} and cross-section A_{tot} is considered. In a 1-D approximation, the specimen is modelled as a discrete arrangement of $N_x \times N_y$ springs, as shown in Fig.1. Each spring is identified by the index pair (i,j), with $i=1\ldots N_x$ and $j=1\ldots N_y$. The specimen is thus discretized in N_x portions, each modelled as an array of N_y parallel springs. Two opposite uniaxial forces of time-varying magnitude $F_{tot}(t)$ are applied at the two ends of the specimen, each undergoing a displacement of magnitude $x_{tot}(t)$ in the direction of the force. In the simplest possible approach, all springs are considered identical in length l and in elastic parameters (Young's modulus E), but their cross-section A_{ij} is allowed to vary within chosen limits, i.e. $A_{min} < A_{ij} < A_{max}$, with the total specimen cross section remaining constant. The stiffness of a single spring can therefore be

written as $k_{ij}=EA_{ij}/l$, whilst the equivalent stiffness of the i-th undamaged material portion, represented by the i-th arrangement of N_y parallel springs, is

$$K_i = \sum_{j=1}^{N_y} k_{ij} .$$ (1)

The length and cross-section of the entire specimen are, respectively:

$$L_{tot} = \sum_{i=1}^{N_x} l_i = N_x l \qquad A_{tot} = \sum_{j=1}^{N_y} A_{ij} \quad (\forall i).$$ (2)

i.e. the cross-section is constant and equal to A_{tot}.
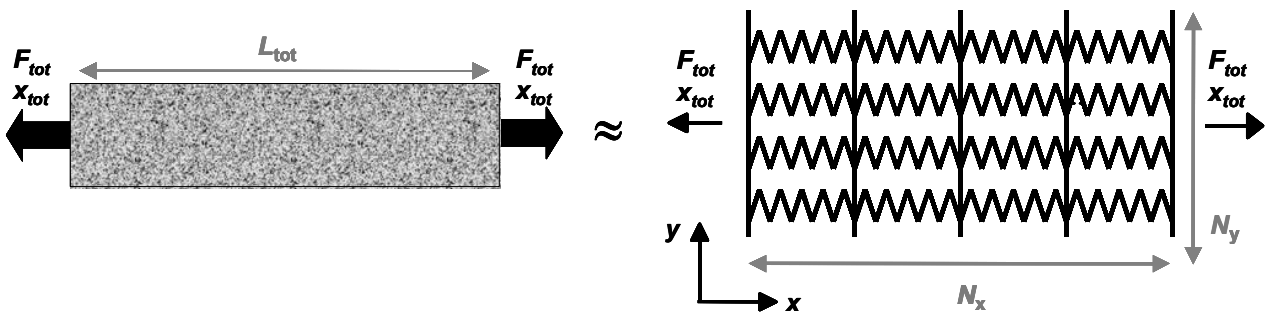
Fig. 1 : Discretization of a specimen subjected to uniaxial tension as adopted in simulations.

Next, a fracture criterion is introduced whereby the failure of the individual spring (i,j) occurs when it undergoes a stress σ_{ij} that exceeds its intrinsic strength σ_{Cij}. The value of σ_{Cij} is assumed to vary from spring to spring and to be distributed randomly, according to the Weibull distribution [5], which is widely used in fracture mechanics. The distribution $P(\sigma_{Cij})$ of the spring strengths can therefore be expressed as:

$$P(\sigma_{Cij}) = 1 - e^{\left[-\left(\frac{\sigma_{Cij}}{\sigma_0}\right)^m\right]} .$$ (3)

where σ_0 is a nominal stress value for the material under investigation, and m is the Weibull modulus, which is characteristic of the considered material. In the model, damage progression is modelled as the failure of the springs used to discretize the specimen. In the case of failure of the (i,j)-th spring, its stiffness k_{ij} is set to zero. It is clear that, as the loading of the specimen increases and the resulting damaging process advances, the stiffness of each section of the material will decrease as fewer and fewer springs forming the section remain intact. Therefore, the stiffness of each section is time dependent, i.e. $K_i = K_i(t)$. Correspondingly, the overall specimen compliance $C(t)$ increases in time. In particular, the overall specimen compliance variation $\Delta C(t)$ deriving from a single spring failure occurring at the location (i,j) can be written as:

$$\Delta C_{ij}(t) = \frac{k_{ij}}{K_i(t)(K_i(t) - k_{ij})} .$$ (4)

The denominator in Eq. (4) indicates that the variation ΔC_{ij} depends on time and on the location of the spring failure taking place, as is intuitive.

The energetic aspects of damage progression are now considered. Energy balance considerations require that the variation of total potential energy $\Delta W_{ij}(t)$ when a spring fails be compensated by the kinetic energy $\Delta T_{ij}(t)$ released in the form of a stress wave generated in the sample. The energetic contribution of the dissipated energy $\Delta \Omega_{ij}(t)$ in the formation of a crack surface at micro- or meso-scale must also be considered. Thus, one can write:

$$\Delta W_{ij}(t) + \Delta T_{ij}(t) + \Delta \Omega_{ij}(t) = 0 .\tag{5}$$

The last term is important in order to obtain the correct scaling properties observed in AE experiments, as discussed below.

One can further observe that in Force-Controlled (*FC*) or Displacement-Controlled (*DC*) quasistatic experiments the potential elastic energy variation for a spring failure can be respectively written as:

$$(FC) \qquad \Delta W_{ij}(t) = -\frac{1}{2} F(t)^2 \Delta C_{ij}(t) \qquad (DC) \quad \Delta W_{ij}(t) = \frac{1}{2} x(t)^2 \Delta K_{ij}(t) .\tag{6}$$

where $\Delta C(t)$ and $\Delta K(t)$ are the specimen compliance and stiffness variations, respectively, due to the spring failure. The dissipated energy $\Delta \Omega$ is assumed to be proportional to the newly created surface A_{ij}:

$$\Delta \Omega_{ij} = G_C A_{ij} .\tag{7}$$

where G_C is the critical strain energy release rate for the material [5]. The above energy contributions can be expressed as a function of the accumulated elastic energy of the (*i,j*)-th spring at failure when the spring failure takes place:

$$\Phi_{ij} = \frac{1}{2} \frac{\sigma_{Cij}^2}{E} A_{ij} l .\tag{8}$$

In the case of quasistatic experiments, it can be assumed as a first approximation that, when a single spring used to discretize the specimen fails, the force acting on the corresponding specimen section will be redistributed evenly among all the adjacent springs. In this mean field approximation, the kinetic released energy can be written, according to the previous equations, as:

$$\Delta T_{ij}(t) = \left(\eta_i(t) - \gamma_{ij} \right) \Phi_{ij} .\tag{9}$$

where:

$$\gamma_{ij} = \frac{2 E G_C}{\sigma_{Cij}^2 l} .\tag{10}$$

and

$$(FC) \qquad \eta_{ij}(t) = \frac{K_i(t)}{K_i(t) - k_{ij}} ; \qquad (DC) \quad \eta_{ij}(t) = \frac{K(t+1)}{K(t)} \frac{K_i(t)}{K_i(t) - k_{ij}} .\tag{11}$$

with $K(t+1)$ and $K(t)$ the total specimen stiffnesses immediately before and after the spring failure, respectively. The dissipated energy can also be expressed by means of the accumulated energy in the (*i,j*)-th spring:

$$\Delta\Omega_{ij} = \gamma_{ij}\Phi_{ij} . \tag{12}$$

Simulation results

As an example, a 1-D specimen is considered in the form of a thin bar of length $L= 10^{-2}$m and cross section $\Sigma=10^{-6}$m^2, discretized by means of a $N_x=1000$, $N_y=1000$ spring arrangement. The chosen material is concrete, with a Young's modulus $E= 23$ GPa, peak stress $\sigma_0= 0.1$ GPa, and Weibull modulus m varying between 1 and 6. To evaluate the influence of the variable spring cross section A_{ij}, two types of simulations are carried out: the first with all the springs having constant cross section ($A_{ij}=A_{tot}/N_y \ \forall i,j$), and the second by assigning random A_{ij} values, with the constraint that the specimen cross section remain constant ($\sum_j A_{ij} = A_{tot}$, $\forall i$).

Firstly, the specimen is subjected to traction with a displacement x_{tot} that increases linearly in time: $x_{tot}=vt$. The objective is to compare the scaling properties for damage progression both when energy dissipation is accounted for and when it is not. The number of failure events, calculated without accounting for energy dissipation and indicated here with N_{AE}, correspond simply to the number of springs undergoing failure because their intrinsic strength is exceeded. A more reliable quantity characterising AE is however the released kinetic energy T.

Figure 2 shows results for a typical numerical experiment with $m=3$. In the case of constant spring cross sections (Fig. 2a), the stress-strain curve displays only some softening before failure occurs. Instead, in the case of randomly varying spring cross sections (Fig. 2b), failure of the whole specimen is reached at a considerably later stage, and softening continues up to decreasing stress values for increasing strain. In the case of constant spring cross section, N_{AE} increases exponentially with time up to failure, as do the released kinetic energy T and the dissipated energy Ω. As discussed in detail elsewhere [6], it is possible to fit the data using a power law dependence, e.g. $N_{AE} \propto t^{\alpha}$, $T \propto t^{\beta}$ where α and β are non-integer exponents that are strongly dependent on the chosen Weibull modulus m. The simulated behaviour is shown in Fig. 2c and 2d: best-fits are obtained for $\alpha = 2.7$ and $\beta = 6.8$ in this case. This fitting procedure supplies the possibility to compare predictions of specific experimental data, and thus derives the most appropriate Weibull modulus value for the material. In the case of variable spring cross sections, the $N_{AE}(t)$ and $T(t)$ plots again display an initial exponential growth, although there is an additional phase where the growth rate decreases and a saturation value is reached before failure, when failure events occur more rarely, and at greater energies.

Different loading protocols are also evaluated: Figures 2e and 2f illustrate the behaviour in the case of cyclic loading with increasing amplitudes. The stress-strain behaviour in this case shows progressive material softening (not shown) with successive cycles and N_{AE} evolves in time with increasing plateaux, as does the released kinetic energy T (Fig. 2f). However, T presents a more marked increase for large t values with respect to N_{AE}, because each spring failure releases a greater energy than released for small t values.

It is of particular interest now to verify the predicted scaling behaviour with specimen dimensions (length, cross-section, and volume) and compare it with experimental results in the literature. Indeed, it was shown in [4] that the number of AE events scales with non-integer exponents smaller than unity, indicating that AE occurs in a fractal domain with dimensions comprised between those of a surface and those of a volume. One therefore assumes:

$$N_{AE}(L_{tot}) \propto L_{tot}^{d_{NL}} ; \qquad N_{AE}(A_{tot}) \propto A_{tot}^{d_{NA}} ; \quad T(L_{tot}) \propto L_{tot}^{d_{TL}} ; \qquad T(A_{tot}) \propto A_{tot}^{d_{TA}} . \tag{13}$$

and proceeds to determine the relevant exponents d_{NL}, d_{NA}, d_{TL}, d_{TA} through simulations. To do this, specimens of different dimensions are considered. In particular, the specimen length L_{tot} is varied between 10^{-6}m and 10^{-2}m (with corresponding discretizations N_x varying between 1 and 1000) and

the cross-section A_{tot} is varied between $10^{-10} m^2$ and $10^{-4} m^2$ (with corresponding discretizations N_y varying between 1 and 1000). Here, results are discussed for constant spring cross-sections only.
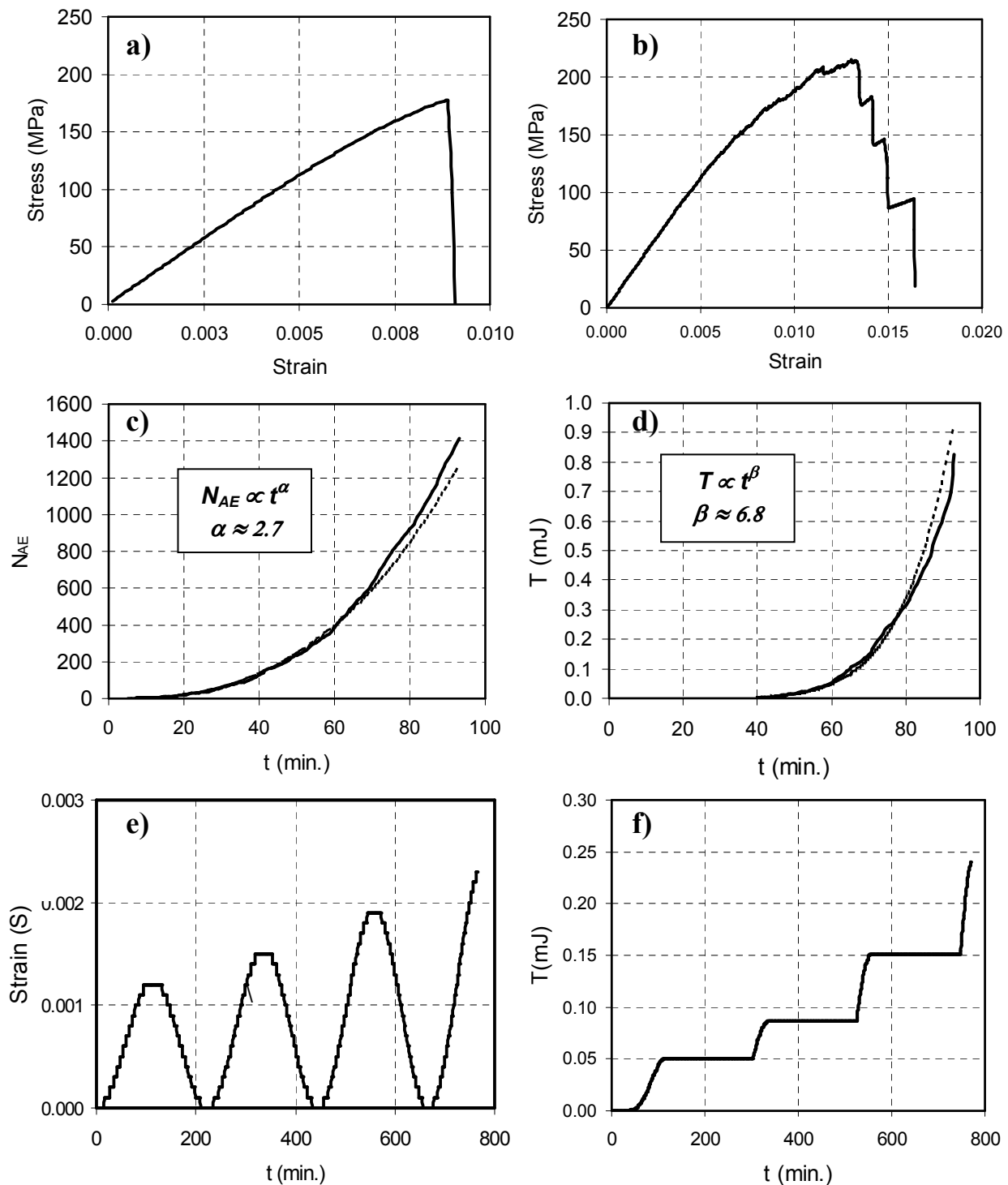
Fig. 2: Simulation results: *(a)* $\sigma(\varepsilon)$ up to failure in the case of constant A_{ij} and $x_{tot}=vt$; *(b)* $\sigma(\varepsilon)$ for random A_{ij} and $x_{tot}=vt$; *(c)* $N_{AE}(t)$ and *(d)* $T(t)$ relative to case *(a)* (fitting power-law functions are also shown). *(e)* $\varepsilon(t)$ and *(f)* $T(t)$ for constant A_{ij} and a periodic loading protocol.

As a uniaxial tensile test is under consideration, one expects L_{tot} to be the relevant dimension with respect to which non-integer scaling occurs. Indeed, the exponents d_{NA}, d_{TA} are on average close to unity after repeated simulations, indicating direct proportionality with respect to specimen cross-section. On the other hand, simulations for different specimen lengths produce average values of $d_{NL}= 0.78$ and $d_{TL}= 0.57$, respectively. Both exponents are consistent with the experimentally derived effect of non-integer exponent scaling. However the latter of the two differs considerably from unity, indicating that the released kinetic energy is a variable that displays the effect to a greater extent, and is therefore a better candidate for comparison with experimentally derived results. This is due to the fact that, when considering T instead of N_{AE}, the dissipated energy is accounted for, as explained above. Figure 3 displays typical results for the T vs. L_{tot} dependence in repeated numerical simulations.
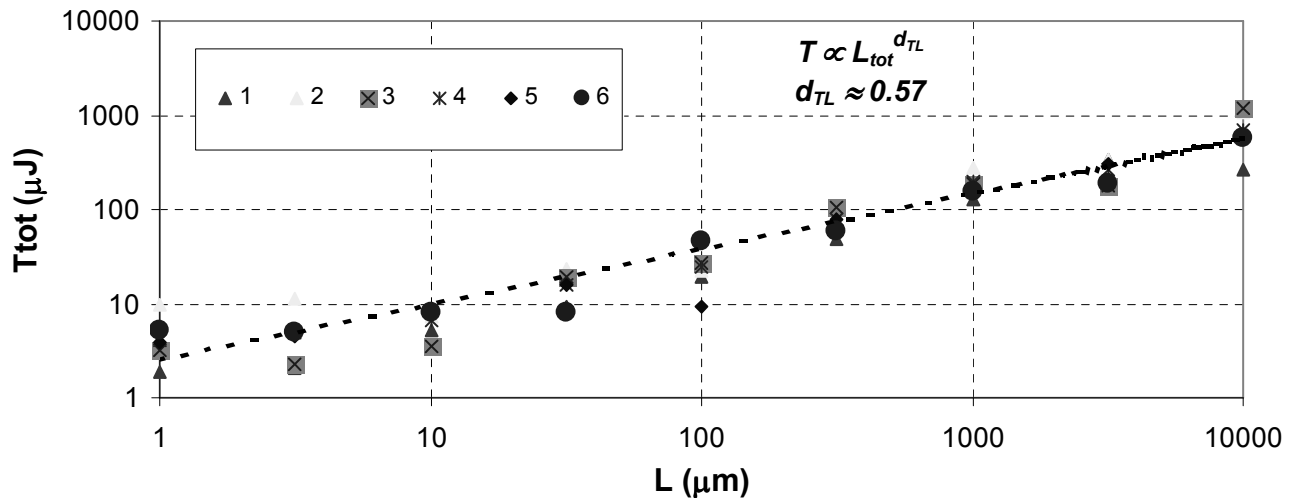
Fig. 3: Scaling properties of AE energy T vs. specimen length L_{tot} in 6 repeated numerical experiments (plot is in log-log scale).

Summary

In conclusion, a simple phenomenological model has been presented that allows to capture a number of important characteristics that emerge in damage progression experiments and AE measurements. In particular, the power law scaling behaviour with respect to specimen dimensions emerges from a correct energetic formulation of fracture events, where part of the stored elastic energy is released in the creation of surfaces at micro/mesoscopic level. Having verified the predictive possibilities of the model, the next step is to compare numerical predictions with specific experimental data both to determine relevant material parameters, verify fitting capabilities and if need be introduce additional elements in the formulation.

References

[1] D.L.Turcotte, W.I.Newman, R.Shcherbakov, Geophys.J.Int. Vol. 152 (2003), p. 718.

[2] S.Zapperi, A.Vespignani, H.E.Stanley, Nature Vol. 388 (1997), p.658.

[3] A.Carpinteri, N.Pugno, Nature Materials Vol. 4 (2005), p. 421.

[4] A.Carpinteri, G.Lacidogna, N.Pugno. Eng. Frac. Mat. Vol. 74 (2007), p.273.

[5] H.J. Hermann, S.Roux, in Statistical models for the fracture of disordered media, Editors H.J. Hermann, S.Roux, Elsevier Science Publishers (North Holland), 1990.

[6] F.Bosia, N.Pugno, G.Lacidogna, A.Carpinteri, submitted for publication (2006)